Shape Optimization with Multiple Loading Conditions and Mesh Refinement

M. E. Botkin*
General Motors Research Laboratories, Warren, Michigan 48090-9057

The capability to handle multiple, static loading conditions has been added to two-dimensional-shape optimization with adaptive mesh refinement. To do this, the mesh refinement portion of the program had to be modified to use the same mesh for all loading conditions. The strain energy density variations for each mesh were normalized, and then maximum values from all loading conditions were used for refinement. Several sample test cases were considered: a two-dimensional bracket with two in-plane loading cases and a folded, stamped-sheet metal part representing an upper suspension control arm and a folded, stamped-sheet metal part representing a brake pedal support bracket. In the case of the two automotive parts, different constraints were active in the two loading conditions indicating that different areas of the structure were being designed by different loading conditions. Converged designs were obtained for the problems considering both loading conditions.

Introduction

THE ability to accommodate multiple loading conditions acting on a structure at different times is a necessity for realistic optimization studies. This capability has been reported in the case of fixed geometry in which the finite element mesh does not change throughout the design iterations. All loading conditions can utilize the same mesh. In the case of shape optimization in which adaptive refinement tailors the mesh differently for each loading condition, a method is needed to use the same mesh for all loading conditions.

A shape optimization capability for stamped-sheet metal components has been described in previous papers.[1,2,3] This approach is based upon a design oriented geometric description consisting of boundary information only. No information about the interior of the structure is used in the definition. Therefore, it was necessary to use a fully automatic mesh generation scheme to create an initially uniform, triangular mesh. After an initial analysis, the mesh is refined within regions of highly varying strain energy density.[4]

The approach described in Ref. 4 will only allow a single static loading condition to be considered. Many realistic mechanical components must be designed for multiple, static loading conditions and in some instances even dynamic loading cases. Many approaches have been proposed and developed for adaptive mesh refinement. Only Shephard[5] has treated the case of multiple loading conditions; although his method has never been used in conjunction with shape optimization.[6] Although the Shephard approach would most likely have been satisfactory to incorporate into a shape optimization procedure, a modified technique was formulated, which was more suitable to the existing mesh refinement capability.

Several design examples are presented to demonstrate the new approach. These problems show that different segments of the boundaries have been designed by different load cases. Furthermore, the refinement, in some cases, increases the stresses so that constraints become active, and hence influence the design, which would otherwise have been ignored thereby resulting in a nonconservative design.

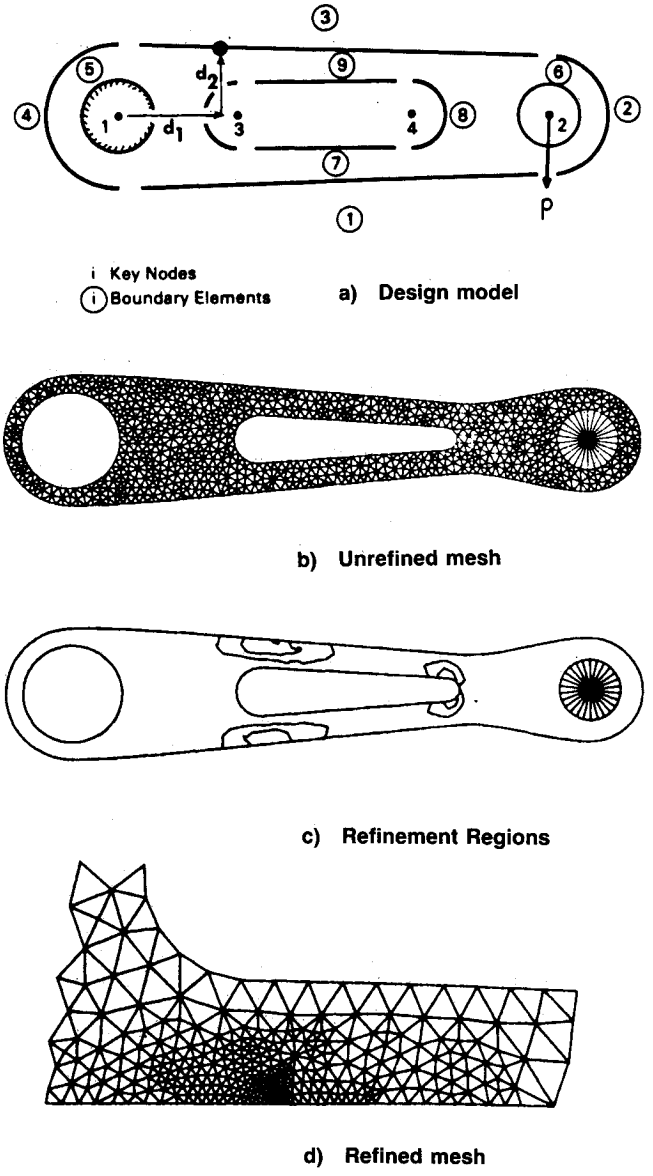

Fig. 1 Boundary design element model and generated meshes.

Received May 5, 1988; revision received Nov. 11, 1988.

*Senior Staff Research Engineer, Engineering Mechanics Department. AIAA Member.

Mesh Generation and Refinement

The need for fully automatic mesh generation within a shape optimization procedure is two fold. First, the design/analysis problem description, in terms of input data necessary to be prepared by the engineer, should be as basic as possible and not redundant. Obviously, since the boundary is what is to be designed then the minimum data required can be provided in terms of mathematical shape functions as shown in Fig. 1a. Second, as the design progresses and the original shape changes, the finite-element mesh should continue to be as adequate as the original mesh. That is to say, no manual improvements should have been made to the original mesh that cannot be made automatically to subsequent meshes. Both of these requirements are satisfied using automatic triangulation as shown in Fig. 1b. A uniform element size must be chosen, which will adequately describe, in a piece-wise linear fashion, the details of the boundary geometry. Once that has been done, the only reason to refine the mesh further is to improve the solution accuracy. It must also be remembered that as the design progresses, the locations requiring refinements for accuracy may also change, due to varying boundary curvatures. For each design iteration, then, the elements must be identified, as shown by the contour regions in Fig. 1c, which need to be refined in order to produce a more accurate solution. There are many approaches for selecting the elements to be refined,[7] but they are all based upon solution quantities obtained from an initial analysis of the unrefined mesh. The relationship between the element size and the error in strain energy density (SED) can be expressed as follows:

$$|E - E_I| < C_j h^k |D^k E|_e \tag{1}$$

in which E is the exact (desired) SED, E_I is the computed value, C_j is a proportionality factor, h is the element size, and D^k is a differential operator of order k (the order of the element). Therefore, for constant-strain elements ($k = 1$), the error is proportional to the element size times the first variation of the SED in the element. The question to be answered, then, is how small should the elements be to produce acceptable errors. Although this question cannot be answered directly, i.e., h in Eq. (1) cannot be computed, a list of elements to be refined can be selected based upon the knowledge gained from Eq. (1). These are the elements with unacceptably large variations in SED. The selection of these elements will be covered in the next section. Once they are known, however, nodes at a refined spacing are added to the mesh, and a new triangulation is obtained as shown in Fig. 1d.

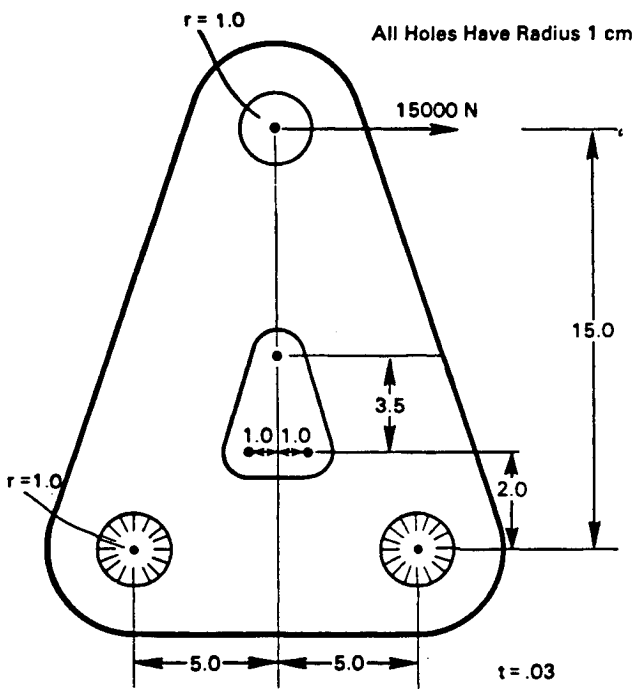

Fig. 2 Triangular bracket example.

Mesh Refinement for Multiple Load Cases

In Ref. 4 an elemental cutoff value (CV) of SED variation (ΔSED) was computed such that any element which had a ΔSED value in excess of CV would be refined:

$$CV = \bar{\Delta E} + \beta(\Delta E_{\max} - \bar{\Delta E}) \tag{2}$$

in which $\bar{\Delta E}$ is the average ΔSED, $\Delta E_{\max}$ is the maximum ΔSED, and β is an input parameter.

In Ref. 5 a single refined mesh is created to be used in the solution of all loading conditions. That approach is also based on refinement of regions in which SED varies rapidly. In order to combine SED values from different loading cases, the elemental values in each case are normalized by the maximum SED value for that case. Since refinement is based upon the SED variation, loading cases with higher variations will have more refinement.

In this paper, a similar procedure is used but with a slight variation. Rather than normalizing the solution by the maximum SED, the solution is normalized by CV for that loading condition. In this way, each load case results in the same refinement region as if it were the only load case. The justification for doing it in this way comes merely from realizing that the refinement approach in Ref. 4 is heuristic, and attempting to weight loading conditions in some way would not have any theoretical justification. Furthermore, using this modified technique should generally give the same localized refinement regions as the individual loading conditions. The result could be thought of as overlaying the SED difference contour plots and using the envelope of all regions. This can be expressed mathematically as follows. For multiple loading conditions, Eq. (2) is still used, but the elemental ΔSED values are modified:

$$\Delta E_i^e = \underset{j}{\overset{nlc}{\text{MAX}}} [\Delta E_{ij}^e / CV_j] \tag{3}$$

Table 1 Loading Conditions

Component	Example 1 L.C. 1	L.C. 2
F_x	15000. N	
F_y		35000. N
F_z		
Component	**Example 2 L.C. 1**	**L.C. 2**
F_x	4450. N	−719. N
F_y	−284. N	−2020.25 N
F_z	1012. N	−88. N
Component	**Example 3 L.C. 1**	**L.C. 2**
F_x	200. N	
F_y	−1000. N	
F_z		−450. N

Table 2 Constants

Value	Example	Example 2 (and example 3)
Thickness	0.3 cm	0.45 cm (0.30 cm)
E	20.74 10^6 N/cm^2	20.74 10^6 N/cm^2
ρ	.00781 kg/cm^3	.00781 kg/cm^3
σ_y	8.0 10^4 N/cm^2	2.1 10^4 N/cm^2
υ	0.25	0.29
Initial mesh size	0.60 cm	0.74 cm

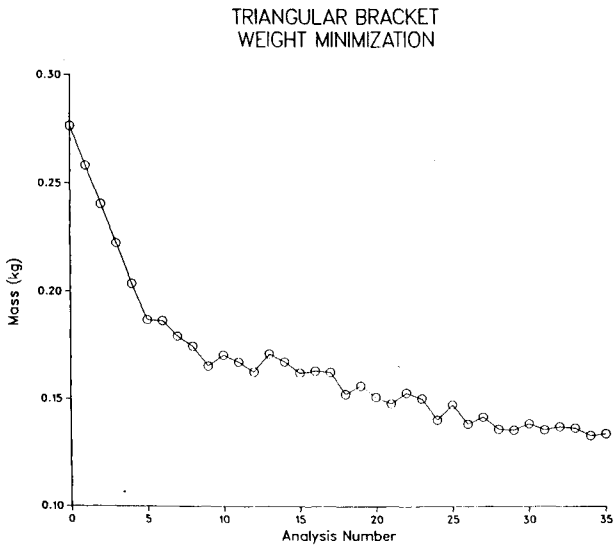

Fig. 3 Mass-iteration history for triangular bracket.

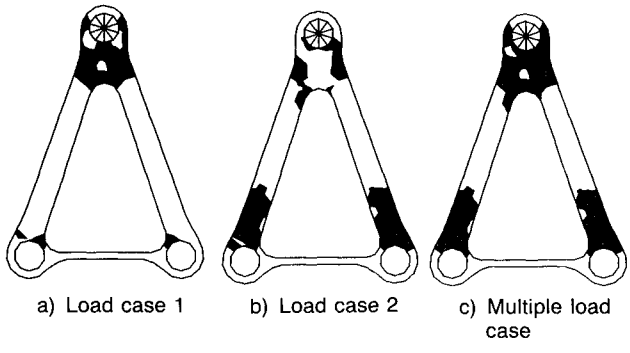

Fig. 4 Comparison of refinement regions for bracket.

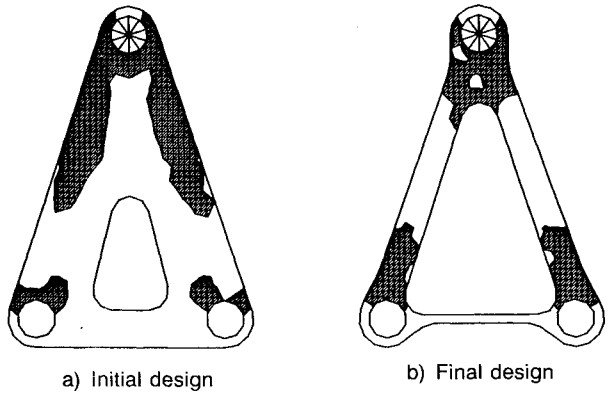

Fig. 5 Initial and final triangular bracket designs.

in which ΔE_i^e is the ΔSED value for element i for all load cases, ΔE_{ij}^e is the elemental ΔSED value for load case j, and CV_j is the ΔSED cutoff value for load case j. If Eq. (3) is used, then $\bar{\Delta E}$ in Eq. (2) is the average of ΔE_i^e, and CV has the value of unity.

The shape optimization capability described in Refs. 1, 2, and 3 was modified to include the above formulation.

Design Examples

The following three problems will be designed for stress conditions only and use adaptive mesh refinement to improve the stress accuracy. The optimization approach uses a sequence of approximate problem solutions in which the subproblem is solved using the CONMIN algorithm. More recent approaches such as mixed variable or force approximation[8] methods could reduce convergence steps to less than 10 but have not been implemented for this study.

Example 1: Triangular Bracket

The triangular bracket shown in Fig. 2 represents a two-dimensional, thin, sheet metal part taken from Ref. 1. In addition to the original, nonsymmetric load previously used, an additional, separate load is applied as given in Table 1. Table 2 gives the constant data. The exterior, initially straight sides, will be allowed to change shape in the form of a double cubic, and the interior cutout will be allowed to change size by varying the key-node locations of the arc boundaries. Design variables are linked to produce symmetry resulting in a total of 6 design variables. For the purpose of demonstration, a uniform mesh size of 0.6 cm will be used.

Table 3 Design data

	Example 1	
Variables	Initial	Final
1	1.000	3.047
2	1.500	1.216
3	5.500	10.379
4	1.500	0.243
5	1.500	1.164
6	1.500	0.904
Mass	.27641	.13368

	Example 2	
Variables	Initial	Final
1	1.500	0.821
2	3.500	1.398
3	2.500	1.201
Mass	.73900	.57512

	Example 3	
Variables	Initial	Final
1	4.000	1.059
2	2.438	1.000
3	1.068	0.500
4	1.000	1.795
5	1.000	2.299
6	14.022	16.371
7	9.986	7.981
8	3.000	3.024
Mass	.57159	.40219

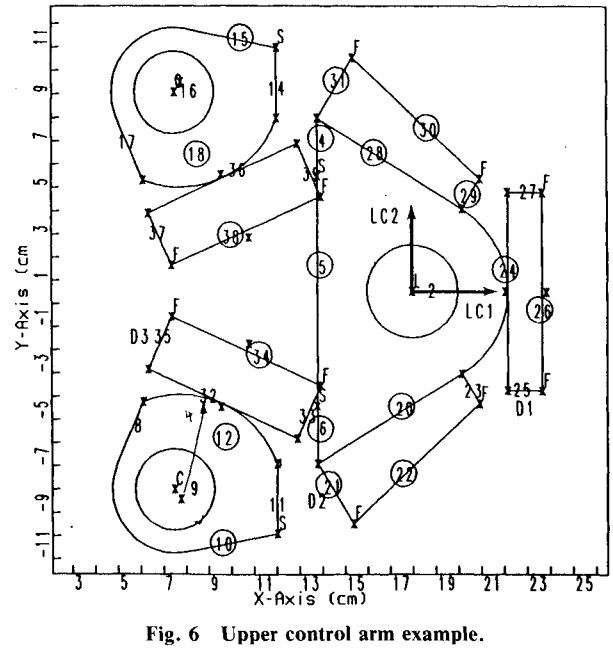

Fig. 6 Upper control arm example.

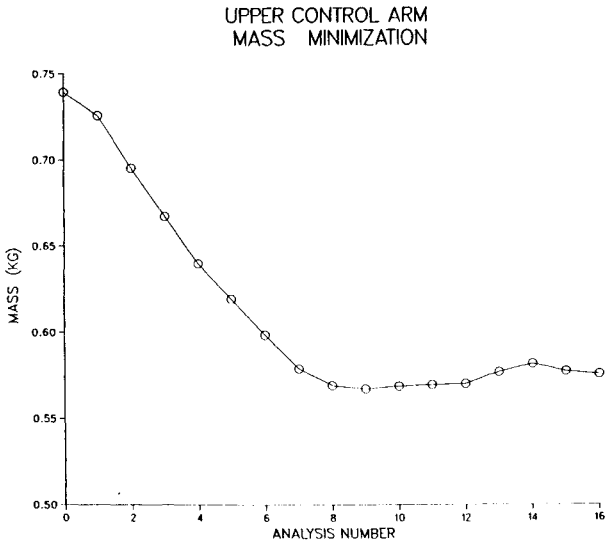

Fig. 7 Mass-iteration history for control arm.

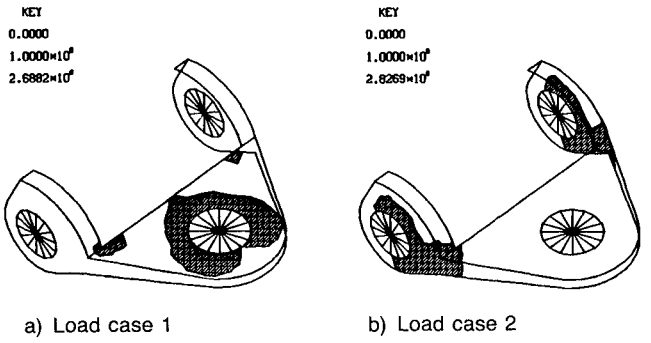

Fig. 8 Comparison of refinement regions for control arm.

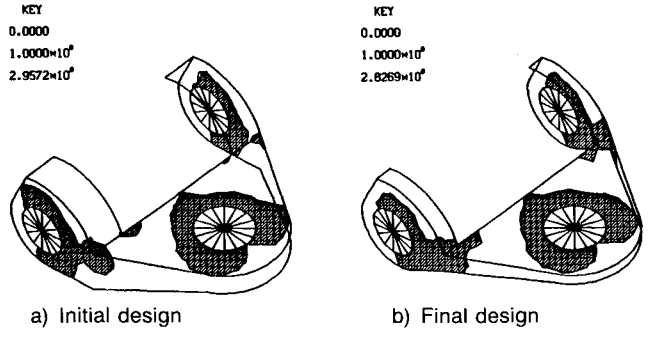

Fig. 9 Initial and final designs for control arm.

Figure 3 shows the mass history for this bracket under these design conditions. Fig. 4 shows the refinement regions for the load case 1 (Fig. 4a), for load case 2 (Fig. 4b) and for the multiple load case (Fig. 4c). It can be seen that the refinement region for the multiple load case is a superposition of the regions of the individual load cases. The initial and final shapes are shown in Fig. 5. Table 3 tabulates the initial and final design data.

Example 2: Upper Control Arm

The part shown in Fig. 6 represents one design alternative for an upper suspension control arm. The two loading conditions used are given in Table 1 and represent a cornering load and a panic brake load. Table 2 gives the constant data. The design will be symmetric and have three design variables. The flanges will be allowed to vary in depth and taper, and the width of the bushing stiffener will vary. These design variables are indicated in Fig. 6 as D1 through D3.

Figure 7 shows the mass history for this bracket under these design conditions. Move limits of 10 % were used for the first 8 steps and then changed to 5 % when unstable oscillations occurred in the convergence. Although the lowest mass was obtained in steps 9–12, constraint violations of > 5 % were encountered, which were satisfied in steps 14–16. Figure 8 shows the refinement regions for the load case 1, for load case 2, and Fig. 9 shows the regions for the multiple load (labeled "Final Design"). It can be seen that the refinement region for the multiple load case is a superposition of the regions of the individual load cases. The initial and final shapes are shown in Fig. 9. Table 3 tabulates the initial and final design data. Table 4 gives the list of active constraints at the final design for the boundaries shown in Fig. 6.

Example 3: Brake Pedal Support Bracket

The part shown in Fig. 10 represents a typical structure which supports an automotive brake pedal. This problem is intended to demonstrate the ability to model only one-half of a symmetric structure and apply the appropriate symmetric and antisymmetric boundary conditions. The two loading conditions given in Table 1 correspond to a symmetric and nonsymmetric case. For the symmetric case, the finite-element nodes along boundary 21 were constrained for the global Z, θ_x, and θ_y coordinates and for the antisymmetric case the global X, Y, and θ_z coordinates were constrained. This means that for constraint evaluations, two finite-element analyses must be performed each with a different boundary condition set. As

Table 4 Active constraints for control arm, > 90 %

Example 2[a]			
L.C. 1	Value	L.C. 2	Value
5	.928	1	.913
6	.935	3	1.000
30	.900	4	1.000
31	.900	5	1.000
		6	.914
		12	.916
		21	.961
		22	.961
		30	.901
		31	.901

[a]These boundary numbers are circled in Fig. 6.

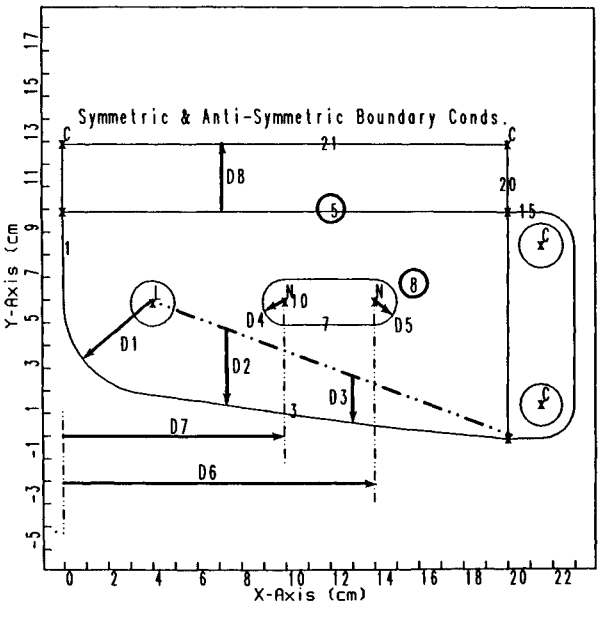

Fig. 10 Brake bracket example.

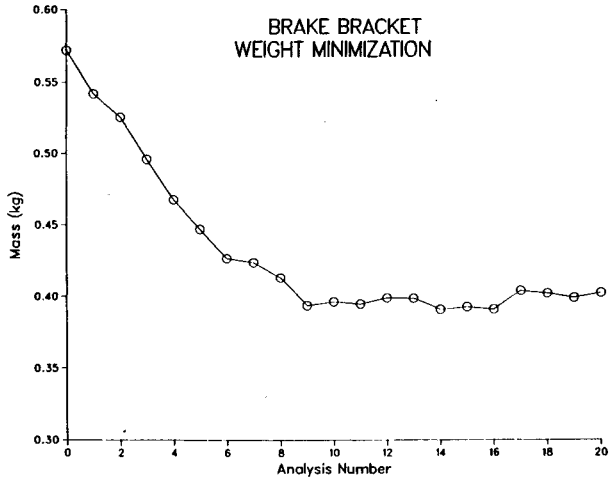

Fig. 11 Mass-iteration history for brake bracket.

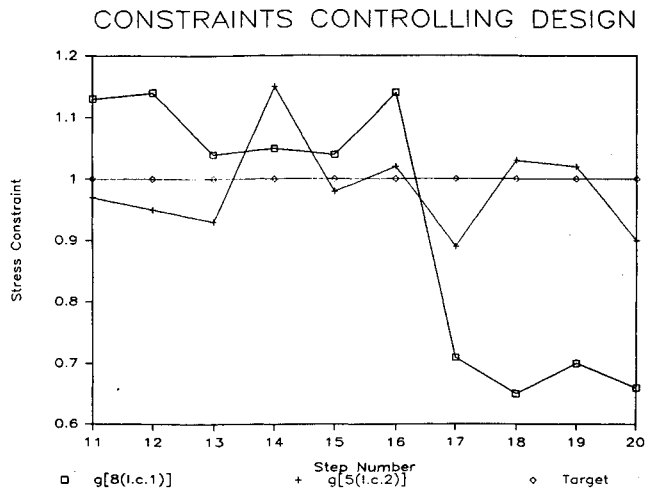

Fig. 13 Controlling constraints for brake bracket.

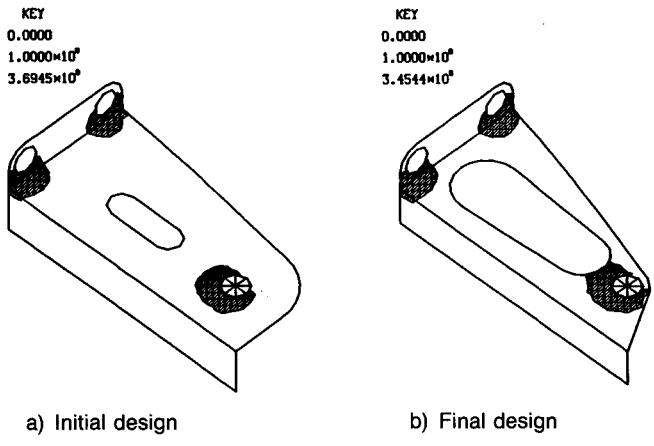

Fig. 12 Initial and final designs for brake bracket.

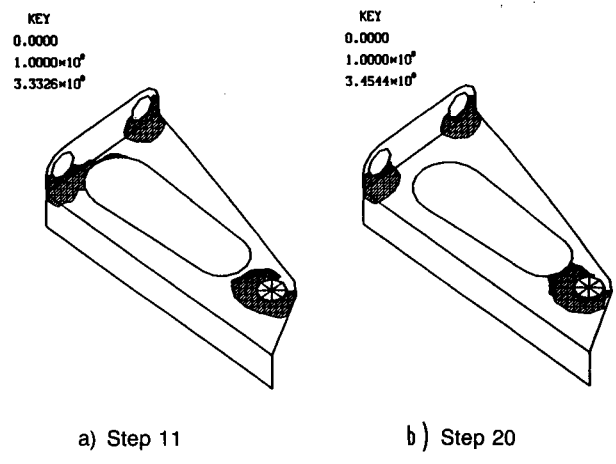

Fig. 14 Refinement regions for Steps 11 and 20.

described before, however, both analyses will be done using the same refined mesh. Table 2 gives the constant data. This problem has 8 design variables indicated by D1 through D8 in Fig. 10, which control the shape of the bottom, curved edge, the size and location of the hole, and the width of the centerline flange. A geometric behavior constraint of 0.3 cm was imposed to keep boundaries from overlapping.

Figure 11 shows the mass iteration history for this bracket. Move limits of 10 % were used for the first 10 steps and then changed to 5 % when unstable oscillations occurred in the convergence. The initial and final shapes are shown in Fig. 12 and initial and final design variables are given in Table 3. The mesh refinement regions are also shown in Fig. 12. Although the lowest mass was obtained in steps 14–16, constraint violations of >10 % were encountered, which were satisfied in steps 17–20. A plot of the maximum constraint value for each loading condition is given in Fig. 13 for the last 10 steps. Figure 14 shows the refinement regions for steps 11 and 20. At step 11 the boundaries for the maximum stress constraints are being refined, i.e., boundaries 5 and 8 (see Fig. 10 for the boundary numbers). In order to satisfy the constraint at boundary 8, the slot is "pushed" away from the end until it is out of the refinement region causing the constraint value to drop (step 17 in Fig. 13). This oscillatory character is typical of shape optimization with mesh refinement.[1,2,3] A few more steps would, most likely, produce a design with both controlling constraints close to unity with a mass in the range between steps 16 and 17. Since this difference is only 3.3% it can be assumed that step 20 is sufficiently close to the optimum.

Generally, for the nonsymmetric case, the active constraints are around the top of the bracket on the boundaries of the connecting flange, which provides the major stiffness in the Z direction. The symmetric loading condition has additional constraints active at the bottom edge of the bracket and around the bottom of the slot. Although the interactions in this type of design problem are quite complicated, it can generally be concluded that the different loading conditions design different areas of the structure or at least have different degrees of influence on the design of a specific area.

Summary

The capability to handle multiple, static, loading conditions has been added to two-dimensional-shape optimization with adaptive mesh refinement. To do this, the mesh refinement portion of the program had to be modified to use the same mesh for all loading conditions. The strain energy density variations for each mesh were normalized and then maximum values from all loading conditions were used for refinement. Several sample test cases were considered: a two-dimensional bracket with two in-plane loading cases and a folded, stamped-sheet metal part representing an upper suspension control arm and a folded, stamped-sheet metal part representing a brake pedal support bracket. In the case of the two automotive parts, different constraints were active in the two load-

ing conditions indicating that different areas of the structure were being designed by different loading conditions. Converged designs were obtained for the problems considering both loading conditions.

References

[1]Bennett, J. A., and Botkin, M. E., "Shape Optimization with Geometric Description and Adaptive Mesh Refinement," *AIAA Journal,* Vol. 23, March 1985, pp. 458-464.

[2]Botkin, M. E., and Bennett, J. A., "Shape Optimization of 3-D Folded Plate Structures," *AIAA Journal,* Vol. 23, Nov. 1985,pp. 1804-1810.

[3]Botkin, M. E., and Gressel, G. S., "A Flange Design Capability for Shape Optimization of Stamped Parts," *SAE Transactions,* Vol. 95, Sec. 4, 1986, pp. 161-170.

[4]Botkin, M. E., "Adaptive Finite Element Mesh Refinement for use with 2-D Shape Optimization," *AIAA Journal,* Vol. 21, May 1985, pp. 812-814.

[5]Shephard, M. S., "An Algorithm For Defining a Single Near-Optimum Mesh For Multiple Load-Case Problems," *International Journal of Numerical Methods in Engineering,* Vol. 15, No. 4, 1980, pp. 617-625.

[6]Bennett, J. A., and Botkin, M. E., ed., *The Optimum Shape: Automated Structural Design,* Plenum Press, New York, 1986.

[7]Zienkiewicz, O. C., and Zhu, J. Z., "A Simple Error Estimator and Adaptive Procedure for Practical Engineering Analysis," *International Journal of Numerical Methods in Engineering,* Vol. 24, 1987, pp. 337-357.

[8]Vanderplaats, G. N., and Salajegheh, E., "A New Approximation Method for Stress Constraints in Structural Synthesis," *Proceedings of the 28th AIAA SDM Conference,* AIAA, New York, 1987, pp. 314-321.